PRELIMINARY ANALYSIS OF LUNAR IMPACT MELT THERMAL SIGNATURES. C. L. Gallinger[1] and R. R. Ghent[1,2], [1]Department of Earth Sciences, University of Toronto, 22 Russell Street, Toronto, Ontario M5S 3B1, Canada (email: cailin.gallinger@mail.utoronto.ca) [2]Planetary Science Institute, 1700 East Fort Lowell, Suite 106, Tucson, Arizona 85719, USA

Introduction: We present preliminary nighttime temperature data for several impact melts on the Moon, as revealed by Diviner thermal infrared radiometry.

The Moon's regolith is largely uniform in thermophysical properties on global scales [1,2], due to the rapidity with which impact gardening homogenizes the lunar surface on timescales <1 Gyr. Important variations exist in the properties of surfaces younger than this, however, which are mainly tied to impact processes that have taken place within this most recent period of the Moon's geologic history. An example of such a contemporary process is the production of impact melts, the remnants of the molten rock ejected during hypervelocity impacts [3]. Impact melts tend to be found in both the interior of craters and on their ejecta surfaces, and exist as either melt sheets that have draped over steep topography or melt pools that have accumulated and cooled in topographic lows [4]. The latter of these constitute important features for understanding the development of lunar regolith, as they record breakdown and accumulation processes happening on fresh, solid rock surfaces on timescales much younger than the youngest volcanic lava flows on the surface of the Moon [5]. Therefore, they can provide unique insight into the early stages of regolith formation, during the transition from solid rock to comminuted fragmental covering.

Impact melts around various large lunar craters have also yielded discordant calculated ages from crater counting studies compared to those calculated for the crater ejecta blankets [6]. The most likely explanation for this is the difference in target strength of the consolidated impact melt vs. the comminuted ejecta blanket, though exact contributions of this effect are not clear [7]. Additionally, it is not known whether the breakdown of impact melts to form regolith happens in a monotonic or non-linear fashion with time; the presence of rocky surfaces at e.g. Tsiolkovskiy crater (age: > 3.2 Ga based on crater counting studies) [8] implies that rocks can continue to be ejected from impact melts on very long timescales, and thus they may not follow the standard evolution and breakdown seen in Copernican impact ejecta [9].

Methods: We analysed the nighttime regolith temperatures on impact melt pools within and around craters 6 km in diameter or larger, and within 45° latitude of the Moon's equator. From an initial list compiled by Neish et al. [10] and Plescia and Cintala [11] this yielded a total of 63 targets, from which we then select areas containing prospective melt pools. The criteria we use for identifying the location of melt pools are: 1) high total power backscatter and high circular polarization ratio (CPR) in Mini-RF radar data, where available [12]; 2) low or near-zero change in elevation over the pool in LOLA 1024 ppd elevation maps; 3) lobate morphologies suggestive of distinct boundaries and evidence of tension cracks, pressure ridges or flow features in LROC NAC high-resolution images [13]; and 4) a consistent average regolith temperature over the whole pool, exclusive of large or very recent and distinctive impact crater ejecta on the pool. We have presently mapped and processed a total of 8 such targets.

Diviner data from channels 6-8 between local times of 1800h and 0600h are obtained using the pfootprint algorithm [14], ensuring that the spacecraft effective field of view (EFOV) lay entirely within the boundaries of the melt pool polygon. Additionally, study area boundaries are selected to be approx. ~5% the diameter of the pool away from its defined edge, in order to exclude heavily bouldered terrain that may have accumulated near the pool edges due to mass wasting, rather than excavation from impacts.

Thermal modelling. We are developing a 1-dimensional thermal model after [1] that incorporates the standard regolith parameters discussed therein, as well as a distinct layer at variable depth to represent the buried impact melt. The thermophysical properties of the buried melt are the same as those used to model ejecta boulders in [15]. The temperature outputs of the model will then be compared to the calculated brightness temperatures and average rock abundances on the melt pools, since the required spatial and local time resolution is not currently available in the PDS. The calculated regolith temperatures will then be compared to thermal model nighttime curves with infinite melt sheet half-spaces at depths of 0-10 cm to determine the thickness of the overlying regolith cover. Below this depth, the variation in surface temperature due to the presence of the buried impact melt is insufficient to be detected at the resolution of Diviner (~1 K change in nighttime temperatures) [16].

Results: The currently-obtained nighttime temperature data are consistent with all mapped melt

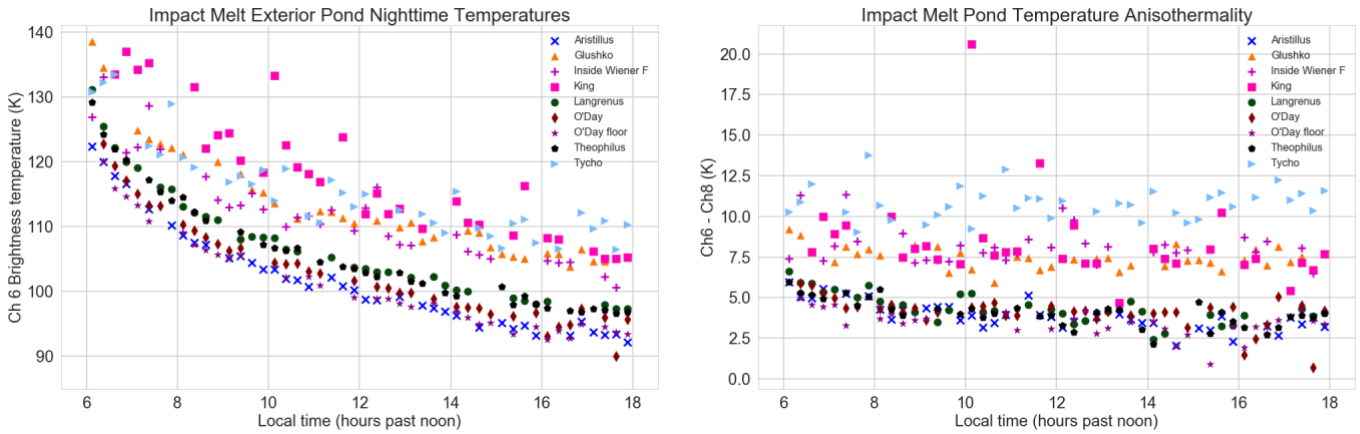

Figure 1: Diviner data from 8 craters with impact melt ponds exterior to their rims, binned and averaged in over 15-minute local time intervals. The ponds at craters such as Tycho, Glushko, King and Wiener F exhibit distinctively higher nighttime temperatures and differences (anisothermality) between the calculated channel 6 and channel 8 brightness temperatures than comparatively older craters such as Langrenus and Theophilus. While exposed surface rocks may account for the anisothermality, buried melt may still be resolvable in the absolute channel brightness temperatures.

ponds having a cover of regolith, as all show steady nighttime cooling. Figure 1 (left) shows the variation in channel 6 brightness temperature for 8 craters counted so far, and figure 1 (right) shows the difference between the channel 6 and channel 8 brightness temperatures caused by the varying temperatures of materials (rocks and regolith) within a single pixel's field of view. This anisothermality is largely due to rocks present at the surface, which cool much more slowly during the lunar night, but cannot be matched and removed using the standard Diviner rock abundance dataset as this is calculated assuming an otherwise typical (i.e. without melt) regolith depth profile [15].

Future work and implications: We will obtain estimates for the thickness of regolith above each of the targeted crater impact melt ponds using the above thermal modelling analysis, and be able to match these to other parameters, such as the crater's published age and rock abundance, in order to resolve relationships between the thermal properties of impact melts and their evolution through time. We expect that, initially, a thin, relatively uniform regolith cover should develop that will obscure the effect of the impact melt below; this may be occurring in the anomalous behavior of O'Day crater in Figure 1, which has a very low minimum nighttime temperature despite being mapped as Copernican in age (and younger than comparatively warmer craters such as Theophilus). Subsequently, infrequent larger impactors may puncture through this fluffy covering and produce blocky ejecta which raise the average temperature of the regolith surface. Finally, in older Copernican and Eratosthenian craters, we expect the nighttime signal will approach that of the background well-mixed regolith covering the majority of the Moon.

Modelling the thermal effects of the presence of buried impact melts could also have many applications to future studies of airless bodies, including deducing the presence of voids or ice layers on comet nuclei and establishing the thickness of thin (<10 cm) regolith coverings on asteroids such as 101955 Bennu, the target of the OSIRIS-Rex mission in 2018.

References: [1] Hayne P. O. et al. (2017) *JGR: Planets, 122,* 1–30. [2] Williams J.-P. et al. (2017) *Icarus, 283,* 300–325. [3] French, B. M. (1998) LPI Contribution No. 954, LPI, Houston, 79–96. [4] Hawke, B.R. and Head, J.W. (1977) In: Roddy, D.J., Pepin, R.O., Merrill, R.B. (Eds.), Permagon Press, New York, NY, 815. [5] Hiesinger H. et al. (2011) *Geol Soc. America Spec. Pap., 477,* 1–51. [6] Hiesinger H. et al. (2012) *JGR, 117,* E00H10. [7] Van der Bogert C. H. et al. (2017) *Icarus, 298,* 49–63. [8] Greenhagen et al. (2016) *Icarus, 273,* 237–247. [9] Ghent R. R. et al. (2014) *Geology, 32,* 12, 1059–1062. [10] Neish C. D. et al. (2014) *Icarus, 239,* 105–117. [11] Plescia J. B. and Cintala M. J. (2012) *JGR, 117,* E00H12. [12] Carter, L. M. et al. (2012) *JGR, 117,* E00H09. [13] Denevi, B. W. et al. (2012) *Icarus, 219,* 665–675. [14] Williams J.-P. et al. (2016) *Icarus, 273,* 205–213. [15] Bandfield et al. (2011) *JGR 116,* E00H02. [16] Paige D. A. et al. (2010) *Space Sci. Rev. 150,* 125.